

# RSC Advances



This is an *Accepted Manuscript*, which has been through the Royal Society of Chemistry peer review process and has been accepted for publication.

*Accepted Manuscripts* are published online shortly after acceptance, before technical editing, formatting and proof reading. Using this free service, authors can make their results available to the community, in citable form, before we publish the edited article. This *Accepted Manuscript* will be replaced by the edited, formatted and paginated article as soon as this is available.

You can find more information about *Accepted Manuscripts* in the [Information for Authors](#).

Please note that technical editing may introduce minor changes to the text and/or graphics, which may alter content. The journal's standard [Terms & Conditions](#) and the [Ethical guidelines](#) still apply. In no event shall the Royal Society of Chemistry be held responsible for any errors or omissions in this *Accepted Manuscript* or any consequences arising from the use of any information it contains.



Journal Name

ARTICLE

## Activation of peroxymonosulfate by BiFeO<sub>3</sub> microsphere under visible light irradiation for decomposition of organic pollutants

Fangli Chi<sup>a†</sup>, Biao Song<sup>a</sup>, Bin Yang<sup>a</sup>, Yaohui Lv<sup>a</sup>, Songlin Ran<sup>a</sup>, Qisheng Huo<sup>b</sup>Received 00th January 20xx,  
Accepted 00th January 20xx

DOI: 10.1039/x0xx00000x

www.rsc.org/

Visible light responsive BiFeO<sub>3</sub> microsphere was successfully synthesized by hydrothermal method and firstly used to activate peroxymonosulfate (PMS) for oxidation and degradation of organic pollutants in water. Rhodamine B (RhB) was used as a model of organic pollutants. It was found that BiFeO<sub>3</sub> reveals high ability to activate PMS that the activated PMS can generate reactive oxidative radicals for further degradation of RhB. In addition, BiFeO<sub>3</sub> exhibited high stability and reusability in degrading organic pollutants through activation of PMS. Here, the comprehensive studies on the kinetics of reaction, PMS concentration and reaction temperature have been done and the possible mechanism was then proposed.

### Introduction

Dyes are widely used in industry in the forms of textile, rubber, paints, leather, paper, plastic, and cosmetic. Huge amount of dyes were released into water every day and this causes serious environmental problems, such as bad smell, colored water, and the increase of toxicity, chemical oxygen demand and biochemical oxygen demand.

Advanced oxidation technologies are considered as an attractive eco-environmental wastewater treatment technology due to the strongly oxidizing radicals like HO<sup>•</sup>, O<sub>2</sub><sup>•-</sup> and OOH<sup>•</sup>. Among these technologies the classic Fenton agent (Fe<sup>2+</sup>, Fe<sup>3+</sup>/H<sub>2</sub>O<sub>2</sub>) is widely used due to its ability to degrade organic pollutants into harmless chemicals such as CO<sub>2</sub> and H<sub>2</sub>O. However, this process is restricted to an environment of low pH (typically 3) and impeded from the follow-up product separation. Recently, peroxymonosulfate (PMS) successfully attracts considerable attention to the environmental applications<sup>1-3</sup> due to its higher oxidizing potential (1.82 V) than H<sub>2</sub>O<sub>2</sub> (1.76 V) as well as its resultant radical species like SO<sub>4</sub><sup>•-</sup> and SO<sub>5</sub><sup>•-</sup> in aqueous medium besides HO<sup>•</sup>. In addition, SO<sub>4</sub><sup>•-</sup> has more selectivity for the oxidation of organic pollutants over a wide pH range, that overcomes some limitations of the conventional Fenton processes. SO<sub>4</sub><sup>•-</sup> can be produced by light (especially UV), transmission metal and heat, in which the method excited by transmission metal is most convenient<sup>5</sup>. Moreover, Co<sup>2+</sup> is very efficient to excite PMS to generate SO<sub>4</sub><sup>•-</sup>, but it is not a good candidate for its incompatibility to the environment. Therefore, scientists are trying to look for new materials or to immobilize Co<sup>2+</sup> on

various supports such as graphene<sup>6</sup>, TiO<sub>2</sub><sup>7</sup>, SiO<sub>2</sub><sup>8</sup>, and Bi<sub>2</sub>O<sub>3</sub><sup>9</sup>. Additionally, Fe<sup>III</sup> has been proved as an effective cation to excite PMS for decolorization of a mono-azo textile dye and acid red 88<sup>10</sup>.

Perovskite-type mixed oxides (ABO<sub>3</sub>) are important heterogeneous catalysts in industrial reactions<sup>11</sup>. In recent years, the interests of multiferroic materials BiFeO<sub>3</sub> with perovskite-type structure have been addressed in the photocatalyst field due to its narrow band-gap energy (2.1 eV-2.9 eV) as well as its high chemical stability<sup>12-14</sup>. For example, Gao et al. have synthesized BiFeO<sub>3</sub> nanoparticles ranging from 80 to 120 nm, and confirmed that the degradation associated with nanoparticles of BiFeO<sub>3</sub> is significantly more efficient than that with bulk BiFeO<sub>3</sub> due to the higher surface area of nano-BiFeO<sub>3</sub><sup>12</sup>. Graphene/BiFeO<sub>3</sub> composites were synthesized by growing BiFeO<sub>3</sub> nanoparticles on graphene sheets to degrade tetrabromobisphenol A, compared with BiFeO<sub>3</sub> the composite presented significantly enhanced visible light Fenton-like catalytic properties due to a large surface area, much increased adsorption capacity and the strong electron transfer ability of graphene in the composite<sup>15</sup>. Furthermore, BiFeO<sub>3</sub> can be used as a heterogeneous Fenton-like catalyst because of its perovskite structure and the content of Fe element. For example, the apparent rate constant for the RhB degradation was very high, which was about 20 folds of that obtained with Fe<sub>3</sub>O<sub>4</sub> nanoparticles as the catalyst under similar conditions<sup>16</sup> when BiFeO<sub>3</sub> nanoparticles were used to degrade Rhodamine B (RhB) with the presence of H<sub>2</sub>O<sub>2</sub>. However, the studies on photocatalyst oxidation of BiFeO<sub>3</sub> with the presence of PMS remain limited. We anticipate that the degradation rate of organic pollutants will increase greatly due to the synergistic effect of visible light photocatalysis and sulfate radical based BiFeO<sub>3</sub>/PMS/Vis system.

In this study, pure BiFeO<sub>3</sub> microsphere with perovskite structure was prepared using hydrothermal method. PMS was introduced in this system, and the catalytic behaviors were

<sup>a</sup> School of Materials Science and Engineering, Anhui University of Technology, Ma'anshan 243002, China

<sup>b</sup> State Key Laboratory of Inorganic Synthesis and Preparative Chemistry, College of Chemistry, Jilin University, Changchun 130012, P. R. China

† E-mail: Flchi12@ahut.edu.cn; Phone/Fax: +86 5552311570

investigated in terms of reaction kinetics, the concentration of PMS and reaction temperature and consequently the degradation mechanism is discussed in the context.

## Results and discussion

The powder X-ray diffraction (XRD) pattern of BiFeO<sub>3</sub> is shown in Fig. 1. The vertical lines at the bottom correspond to the standard XRD pattern of orthorhombic BiFeO<sub>3</sub> (JCPDS 74-2016). As shown in the patterns, all the diffraction peaks can be assigned to the pure phase of BiFeO<sub>3</sub> and no noticeable peaks from other phases were detected. This demonstrates that single phase BiFeO<sub>3</sub> has been successfully obtained under these conditions. The morphologies of the BiFeO<sub>3</sub> sample were examined using SEM, as shown in Fig. 2(a). BiFeO<sub>3</sub> exhibits well-defined microsphere morphology, which diameter is about 16  $\mu\text{m}$ . It can be seen from Fig. 2(b) that the BiFeO<sub>3</sub> powders are composed of irregular segments.

The UV-Vis diffuse reflectance spectra of BiFeO<sub>3</sub> microsphere is shown in Figure 3, in which the inserted graph is the Tauc's plot (an UV-Vis absorption spectrum),  $(\alpha h\nu)^2$  vs  $h\nu$ . The calculated optical band gap of the BiFeO<sub>3</sub> microsphere is 1.92 eV. BiFeO<sub>3</sub> microsphere can effectively absorb considerable amounts of visible light that suggests the potential applications as visible-light driven photocatalysts. In addition, a secondary edge that can be also observed at higher wavelengths. The obvious shift in absorption edge of the sample may be caused by the morphology of sample<sup>17</sup>.

RhB was chosen as a model of organic pollutants<sup>18</sup>. Fig. 4(a) shows RhB was degraded at different conditions. The initial concentration of RhB is defined as  $C_0$  while  $C$  is referred to the instantaneous concentration of RhB at different time. The  $C/C_0$

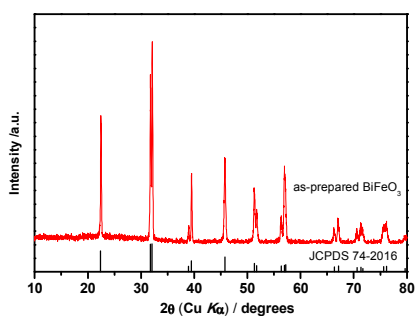


Fig.1. X-Ray diffraction pattern of BiFeO<sub>3</sub> microsphere.

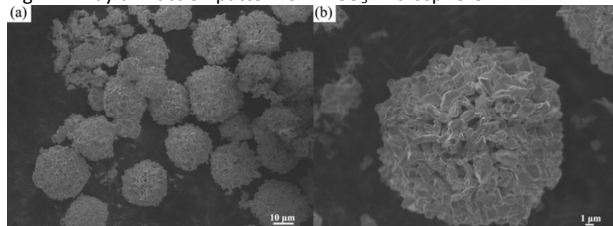


Fig.2. SEM images of BiFeO<sub>3</sub>.

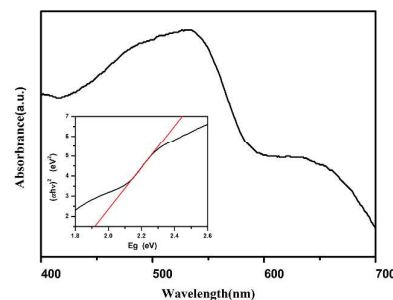


Fig.3. UV-Vis absorption spectra of BiFeO<sub>3</sub> microsphere; inset diagram indicates its calculated band gap.

values of BiFeO<sub>3</sub> only, PMS only, BiFeO<sub>3</sub> and PMS are 97.5%, 52.9%, 37.0% at the 40<sup>th</sup> minute of the reaction time. This result suggested that: a) BiFeO<sub>3</sub> exhibits efficient photocatalytic activity under visible-light irradiation, which has been confirmed in literatures<sup>12, 19</sup>. b) PMS itself can directly oxidize RhB in water under the visible light. This is because PMS can generate  $\text{SO}_4^{\bullet-}$  which has strong oxidation ability. c) BiFeO<sub>3</sub> can accelerate the degradation of RhB in the presence of PMS, it is more than 25 times faster than that caused by BiFeO<sub>3</sub> itself. Fig. 4(b) shows the UV-Vis spectral changes of RhB in the presence of BiFeO<sub>3</sub> and PMS. The intensity of the absorption peak of RhB at 554nm decreases with time very quickly and this indicates the destruction of chromophoric structure of RhB<sup>20</sup>.

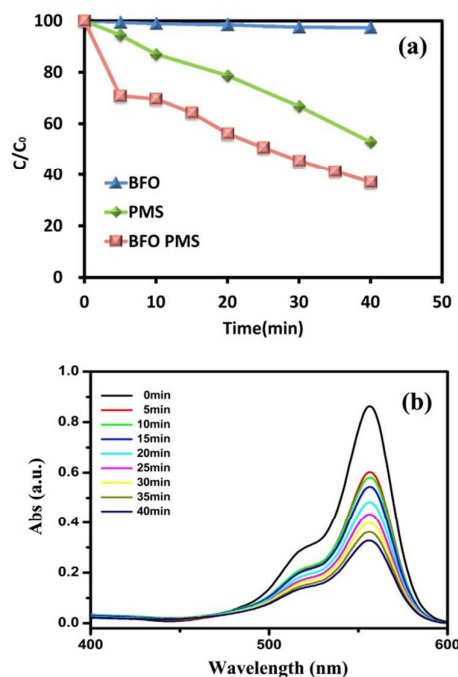


Fig.4. (a) RhB degradation under different conditions. (b) UV-Vis absorbance curves of degraded RhB solutions over the BiFeO<sub>3</sub>/PMS under visible light irradiation. Reaction condition: [RhB] = 5mg/L, [PMS] = 5mM, [BiFeO<sub>3</sub>] = 1g/L, reaction temperature = 25°C.

### Effect of PMS concentration

In order to evaluate the effect of PMS concentration on the decolorization of RhB, a series of experiments were carried out by varying the concentration of PMS from 0 mM to 7 mM while keeping the other experimental parameters constant. As shown in Fig. 5(a), the  $C/C_0$  values are 97.5%, 81.5%, 53.3%, 37.0% and 6.2% for the concentration of PMS at 0 mM, 1 mM, 3 mM, 5 mM and 7 mM, respectively. These observations indicate that the higher initial PMS concentration, the faster degraded RhB. The kinetic study of photocatalytic degradation of RhB was also investigated and fitted by first order reaction kinetic model, as shown in Fig. 5(b). The rate constant of the RhB degradation 0 mM, 1 mM, 3 mM, 5 mM is estimated to be 0.0007, 0.0043, 0.016, 0.026  $\text{min}^{-1}$ , respectively. The corresponding  $R^2$  (correlation coefficient) values are 0.958, 0.943, 0.912 and 0.916, respectively, which are close to 0.99, proving that the photocatalytic reaction is in line with the proposed rate law for RhB degradation. The results are similar to that of  $\text{MnFe}_2\text{O}_4$ , which is also used as catalysts to activate PMS to degrade organic pollutants<sup>21</sup>. For PMS 5 mM the corresponding degradation rate constant of RhB is about 1.6-fold faster than that of PMS 3 mM, for PMS 3 mM the corresponding degradation rate constant of RhB is about 3-fold faster than that of PMS 1 mM, indicating the ratio of rate constant is nearly equal to the ratio of specific concentration of PMS.

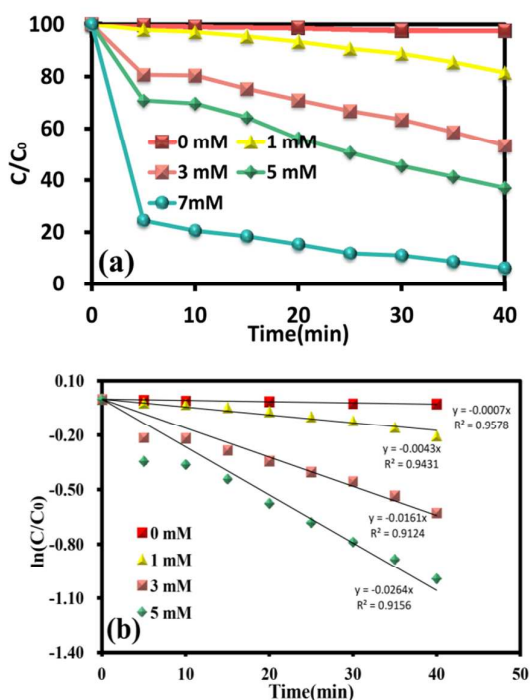


Fig.5. (a) Effect of PMS concentration on the removal of RhB by  $\text{BiFeO}_3/\text{PMS}$  processes. (b) Kinetic curves of RhB removal in the presence of different concentration of PMS. Experimental conditions:  $[\text{RhB}] = 5 \text{ mg/L}$ ;  $[\text{BiFeO}_3] = 1 \text{ g/L}$ ; reaction temperature =  $25^\circ\text{C}$ .

### Effect of reaction temperature

The effect of reaction temperature was also evaluated by carrying out several experiments with varying reaction temperatures from  $25^\circ\text{C}$  to  $45^\circ\text{C}$ . As shown in Fig. 6(a), the degradation rate of RhB could reach 30% in 5 min at  $25^\circ\text{C}$ , while it could be 77% in 5 min at  $45^\circ\text{C}$ . It was observed that higher temperature facilitates higher degradation efficiency of RhB during the same period. This is because high temperatures could increase the energy absorption for the O–O break, which would generate more sulfate radicals<sup>22</sup>.

### Reusability of $\text{BiFeO}_3$

Photocatalyst reusability is an important factor for its practical application. To investigate the reusability of  $\text{BiFeO}_3$  in PMS system, several repeated photocatalytic experiments were conducted under the same reaction conditions. The removal of RhB could still reach 61% within 40 min, as shown in Fig. 7, after three consecutive cycle runs, which indicates that the photocatalytic efficiency consistently remained high. Figure 8 (XRD analysis) also illustrated that the crystal structure of the  $\text{BiFeO}_3$  photocatalysts did not change after the photo-catalytic reaction. Therefore,  $\text{BiFeO}_3$  can be regarded as stable photocatalyst in the experiments.

### Possible mechanism

In order to confirm the contribution of the oxidizing radical species, three scavengers ethanol (EtOH), t-butanol (t-BuOH) and 1,4-benzoquinone (BQ) were employed. EtOH is capable of

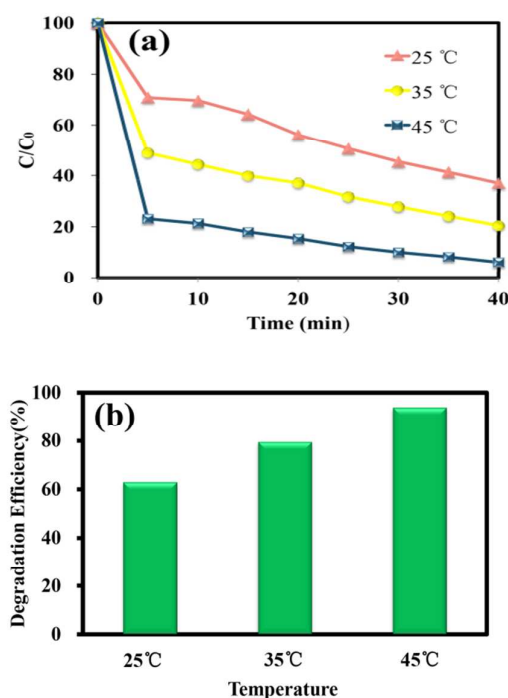


Fig.6. (a) Effect of reaction temperature on the removal of RhB by  $\text{BiFeO}_3/\text{PMS}$  processes. (b) Degradation efficiency of RhB at different temperature. Experimental conditions:  $[\text{RhB}] = 5 \text{ mg/L}$ ,  $[\text{BFO}] = 1 \text{ g/L}$ ,  $[\text{PMS}] = 5 \text{ mM}$ .

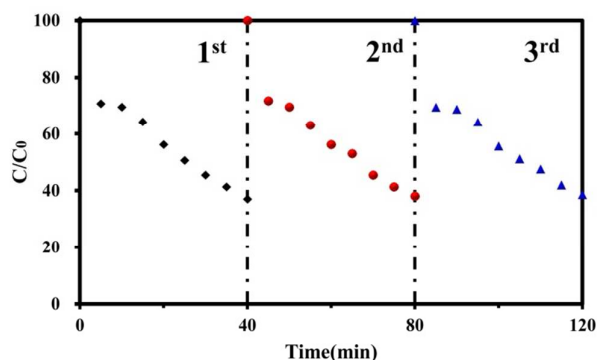


Fig. 7. Reusability of BiFeO<sub>3</sub>. Experimental conditions: [RhB] = 5 mg/L; [BiFeO<sub>3</sub>] = 1g/L; reaction temperature = 25 °C.

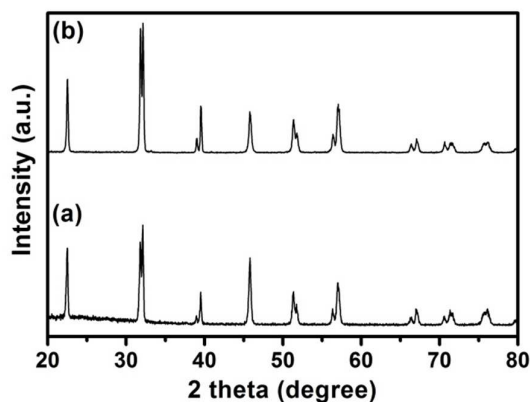
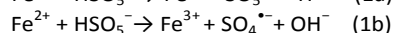
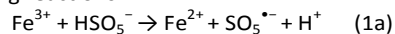


Fig. 8. XRD patterns of the BiFeO<sub>3</sub> (a) after and (b) before the cycling photocatalytic experiments.

quenching sulfate as well as hydroxyl radicals because it has a high reactivity towards both radicals. Whereas t-BuOH mainly reacts with hydroxyl radical and much slowly with sulfate radical<sup>23</sup>, BQ was used as O<sub>2</sub><sup>•-</sup> quencher<sup>24</sup>. About 88.3% RhB is found degraded after 60 min when no quenching agent was added, as shown in Fig. 9. However, the addition of 1M t-BuOH or EtOH brought ~36.4% reduction (from 88.3 to 51.9 %) or ~46.0% reduction (from 88.3 to 42.3 %) in the degradation of RhB at 60th min, respectively. The results suggest that the main generated radical species during the activation of PMS by BiFeO<sub>3</sub> are HO<sup>•</sup> and SO<sub>4</sub><sup>•-</sup> radicals.

The O<sub>2</sub><sup>•-</sup> radical may also play an important role in the degradation of RhB. Fig. 9 shows that the addition of 5mM BQ resulted in a 20.0% drop of RhB degradation. However, no significant decrease is observed during the first 20 mins. The result indicates the delayed formation of O<sub>2</sub><sup>•-</sup> during the reaction.

Previous study<sup>25, 26</sup> shows that the homogeneous Fe<sup>3+</sup>/PMS system could produce SO<sub>4</sub><sup>•-</sup> as the main oxidation species by the following reactions:



Combining our experimental results with the data of homogeneous Fe<sup>3+</sup>/PMS system in the literature, the possible

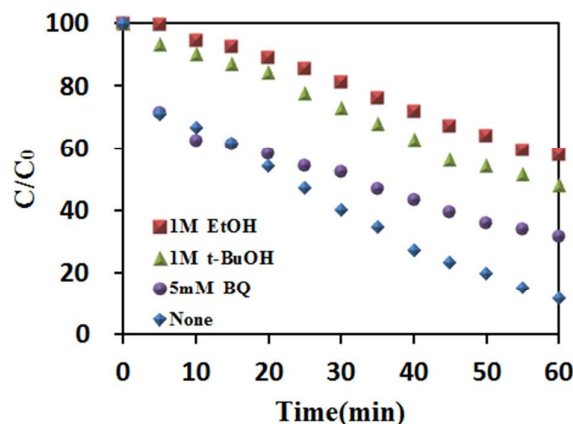
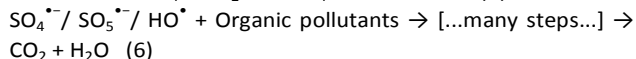
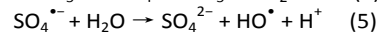
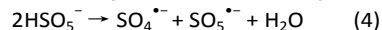
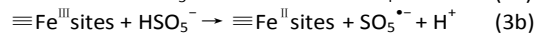
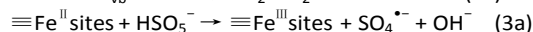
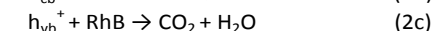
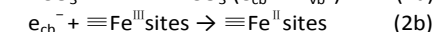
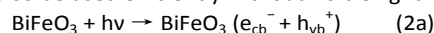


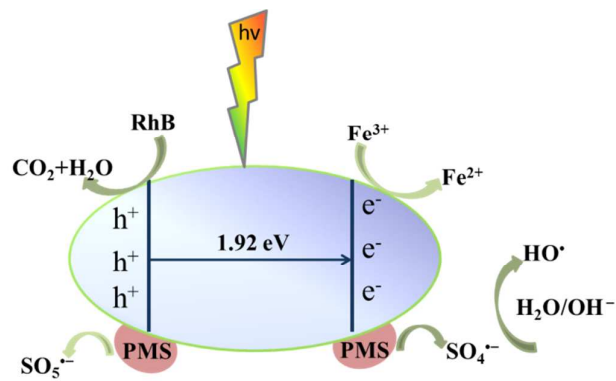
Fig. 9. Effect of radicals scavengers on the degradation of RhB ([PMS] = 3.0mM, [catalyst] = 1.0g/L, t = 30 °C)

activation mechanism of PMS by BiFeO<sub>3</sub> under visible light was suggested (Scheme 1). BiFeO<sub>3</sub> with narrow band-gap energy (1.92 eV) could be easily excited by visible light. The valence band potential (E<sub>VB</sub>) and the conduction band potential (E<sub>CB</sub>) are 2.35 eV and 0.43 eV (vs.NHE), respectively, based on empirical equation<sup>27, 28</sup>. Photo-generated electrons can react with Fe<sup>III</sup> and photo-generated holes can react with RhB directly (Eqns. (2a), (2b) and (2c)). Meanwhile, Fe<sup>III</sup> and Fe<sup>II</sup> can also excite PMS to generate SO<sub>4</sub><sup>•-</sup> and SO<sub>5</sub><sup>•-</sup> (Eqns. (3a) and (3b)). Hence, Eqn. (4) can be derived from Eqn. (3a) and (3b). From Eqn. (4), no presence of Fe<sup>III</sup> indicates that the role of Fe<sup>III</sup> is a recycling catalyst. Furthermore, SO<sub>4</sub><sup>•-</sup> can react with H<sub>2</sub>O/OH<sup>-</sup> to generate HO<sup>•</sup> (Eqn.(5))<sup>29</sup>. Therefore, BiFeO<sub>3</sub>/PMS system can generate radical to degrade organic pollutants efficiently under visible light irradiation, the mechanism can be expressed briefly by Eqns.6. It is worth mentioning that this system can also be used efficiently without visible light.



## Conclusions

In summary, BiFeO<sub>3</sub> microsphere has been successfully synthesized by hydrothermal method. BiFeO<sub>3</sub> demonstrates higher catalytic activity to activate PMS and results in SO<sub>4</sub><sup>•-</sup> and SO<sub>5</sub><sup>•-</sup> under visible light and it can also accelerate the degradation rate of RhB, which is nearly two times with the presence of PMS than the rate in the system of only PMS itself. The more PMS used, the faster reaction rate produced, the ratio of rate constant is nearly equal to the ratio of specific concentration of PMS. Higher reaction temperature is also



Scheme 1. Mechanism for RhB degradation by BiFeO<sub>3</sub>/PMS/Vis system

better for the degradation of RhB. A suitable mechanism is suggested to explain the observed photocatalyzed degradation of RhB. These results demonstrate that BiFeO<sub>3</sub>/PMS behaves as an efficient material in photocatalytic oxidation of organic pollutants.

## Experiment

### Synthesis of BiFeO<sub>3</sub>

BiFeO<sub>3</sub> was fabricated by hydrothermal method. In a typical synthesis, 0.1 mol Fe(NO<sub>3</sub>)<sub>3</sub>·9H<sub>2</sub>O and 0.1 mol Bi(NO<sub>3</sub>)<sub>3</sub>·5H<sub>2</sub>O were used as raw materials and were dissolved in 15 mL of distilled water, the amount of KOH was added as a mineralizer, after stirring for half an hour, the brown suspension were transferred into Teflon-lined stainless steel autoclave, the autoclave was then sealed and heated at 200 °C for 6 h. After cooling to room temperature naturally, the precipitates were collected by vacuum filtration and washed with distilled water until a pH of 7 was obtained. Then, the produced powder was dried at room temperature.

### Catalytic degradation experiments

Photocatalytic activities of the samples were evaluated by the degradation of RhB with a 500 W xenon (Xe) lamp, which positioned in a quartz cold trap with flowing cold water to avoid overheat caused by lamp long time irradiation. The cutoff filters ( $\lambda \geq 420$  nm) were used to remove radiation below 420 nm. The degradation experiments were carried out in a cylindrical Pyrex vessel (250 mL). The vessel with 200 mL RhB (5 mg L<sup>-1</sup>) solution was put into the thermostatic oil bath (increased to and kept at the reaction temperature) and kept stirring for 30 min to insure the RhB solution reach the desired temperature, then 0.2 g of BiFeO<sub>3</sub> was dispersed into RhB solution and magnetically stirred in the dark for 30 min to insure the adsorption-desorption equilibrium between the dye and photocatalyst. A certain amount of PMS was added to the reactor, and the lamp was turned on immediately to initiate the photocatalytic oxidation reactions. Once PMS meets dye in water, dye concentration will decrease quickly. The concentration of RhB solution was monitored by measuring

the absorbance at 554 nm and taken the initial concentration as C<sub>0</sub>. After the elapse of a period of time, 4 ml of the solution was taken and filtered by the 0.22  $\mu$ m membrane in order to separate the catalyst powders from the solution, where the instantaneous concentration of RhB was measured at different time as C.

In the recycling experiments, the solution was deposited for about one hour to avoid the loss of the catalyst and the precipitate was centrifuged to collect the photocatalyst after the added RhB was almost degraded. It was washed with deionized water as well as ethanol for several times and then dried at room temperature. Then the final products were suspended in a fresh solution of RhB and PMS, followed by RhB degradation as the second cycle. This process was repeated as the third cycle.

To confirm the contribution of the oxidizing radical species, ethanol (EtOH), t-butanol (t-BuOH) and 1,4-benzoquinone (BQ) were employed as radical scavengers. Quenching experiments were performed by adding the scavengers into the reaction solution before the participation of PMS.

### Catalyst characterization

The crystal structure of dried powders was characterized from the X-ray powder diffraction (XRD) patterns using a Rigaku D/MAX 2550 diffractometer with Cu K $\alpha$  radiation ( $\lambda = 1.5418$  Å). Scanning electron microscopy (SEM) images were taken by a JEOL JSM-6700F microscope at 10 kV. The UV-Vis absorption spectra of the samples were measured using TU-1901 ultraviolet / visible optical absorption spectrometry. UV-Vis diffuse reflectance spectroscopic (DRS) studies were carried out using a Shimadzu UV-3600 equipped with an integrating sphere at the room temperature in air, and BaSO<sub>4</sub> was used as the reference material.

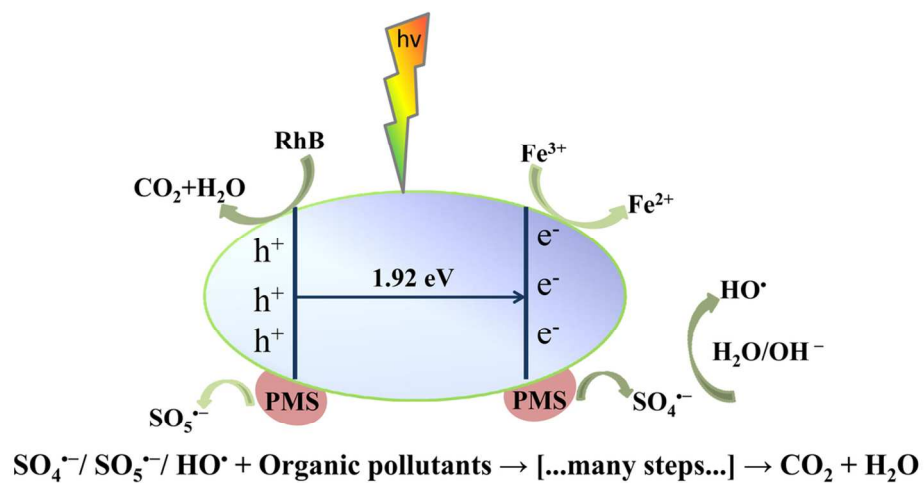
## Acknowledgements

This work was supported by Open Research Fund Program of State Key Laboratory of Inorganic Synthesis and Preparative Chemistry (No. 2014-31) and Youth Foundation of Anhui University of Technology.

## References

- 1 L. J. Xu, W. Chu and L. Gan, *Chem Eng J*, 2015, **263**, 435-443.
- 2 W.-D. Oh, S.-K. Lua, Z. Dong and T.-T. Lim, *J Hazard Mater*, 2015, **284**, 1-9.
- 3 J. Liu, Z. Zhao, P. Shao and F. Cui, *Chem Eng J*, 2015, **262**, 854-861.
- 4 Y. M. Ren, L. Q. Lin, J. Ma, J. Yang, J. Feng and Z. J. Fan, *Appl Catal B-Environ*, 2015, **165**, 572-578.
- 5 S. L. Luo, L. Duan, B. Z. Sun, M. Y. Wei, X. X. Li and A. H. Xu, *Appl Catal B-Environ*, 2015, **164**, 92-99.
- 6 Y. Yao, Z. Yang, H. Sun and S. Wang, *Industrial & Engineering Chemistry Research*, 2012, **51**, 14958-14965.
- 7 Y. Zhu, S. Chen, X. Quan and Y. Zhang, *Rsc Adv*, 2013, **3**, 520-525.
- 8 L. Hu, X. Yang and S. Dang, *Applied Catalysis B: Environmental*, 2011, **102**, 19-26.
- 9 Y. Ding, L. Zhu, A. Huang, X. Zhao, X. Zhang and H. Tang, *Catalysis Science & Technology*, 2012, **2**, 1977-1984.

- 10 J. Madhavan, P. Maruthamuthu, S. Murugesan and S. Anandan, *Applied Catalysis B: Environmental*, 2008, **83**, 8-14.
- 11 R. Spiniccia, M. Faticantib, P. Marinia, S. De Rossib and P. Portab, *Journal of Molecular Catalysis A: Chemical*, 2003, **197**, 147-155.
- 12 F. Gao, X. Y. Chen, K. B. Yin, S. Dong, Z. F. Ren, F. Yuan, T. Yu, Z. G. Zou and J. M. Liu, *Adv Mater*, 2007, **19**, 2889-2892.
- 13 T. Choi, S. Lee, Y. J. Choi, V. Kiryukhin and S. W. Cheong, *Science*, 2009, **324**, 63-66.
- 14 Y. N. Huo, M. Miao, Y. Zhang, J. A. Zhu and H. X. Li, *Chem Commun*, 2011, **47**, 2089-2091.
- 15 J. J. An, L. H. Zhu, N. Wang, Z. Song, Z. Y. Yang, D. Y. Du and H. Q. Tang, *Chem Eng J*, 2013, **219**, 225-237.
- 16 W. Luo, L. Zhu, N. Wang, H. Tang, M. Cao and Y. She, *Environ Sci Technol*, 2010, **44**, 1786-1791.
- 17 S. Li, Y. H. Lin, B. P. Zhang, Y. Wang and C. W. Nan, *J Phys Chem C*, 2010, **114**, 2903-2908.
- 18 Y. Cui, Z. Ding, P. Liu, M. Antonietti, X. Fu and X. Wang, *Phys Chem Chem Phys*, 2012, **14**, 1455-1462.
- 19 S. Li, J. M. Zhang, M. G. Kibria, Z. T. Mi, M. Chaker, D. L. Ma, R. Nechache and F. Rosei, *Chem Commun*, 2013, **49**, 5856-5858.
- 20 K. Wangkawong, D. Tantraviwat, S. Phanichphant and B. Inceesungvorn, *Appl Surf Sci*, 2015, **324**, 705-709.
- 21 Y. Yao, Y. Cai, F. Lu, F. Wei, X. Wang and S. Wang, *Journal of Hazardous Materials*, 2014, **270**, 61-70.
- 22 D. Chen, X. Ma, J. Zhou, X. Chen and G. Qian, *Journal of Hazardous Materials*, 2014, **279**, 476-484.
- 23 P. Shukla, S. Wang, K. Singh, H. M. Ang and M. O. Tadé, *Applied Catalysis B: Environmental*, 2010, **99**, 163-169.
- 24 C. Cai, H. Zhang, X. Zhong and L. W. Hou, *J Hazard Mater*, 2015, **283**, 70-79.
- 25 G. P. Anipsitakis and D. D. Dionysiou, *Environ Sci Technol.*, 2004, **38**, 3705-3712.
- 26 W. Eerenstein, N. D. Mathur and J. F. Scott, *Nature*, 2006, **442**, 759-765.
- 27 H. Dong, G. Chen, J. Sun, Y. Feng, C. Li, G. Xiong and C. Lv, *Dalton T*, 2014, **43**, 7282-7289.
- 28 S. Mukhopadhyay, I. Mondal, U. Pal and P. S. Devi, *Physical Chemistry Chemical Physics*, 2015, DOI: 10.1039/C5CP02689J.
- 29 H. Lin, J. Wu and H. Zhang, *Chem Eng J*, 2014, **244**, 514-521.



BiFeO<sub>3</sub> microsphere was firstly used to activate peroxydisulfate under visible light irradiation for oxidation and degradation of organic pollutants.  
55x30mm (600 x 600 DPI)